

See discussions, stats, and author profiles for this publication at: <https://www.researchgate.net/publication/7484245>

# Parallel Synthesis and High Throughput Dissolution Testing of Biodegradable Polyanhydride Copolymers

ARTICLE *in* JOURNAL OF COMBINATORIAL CHEMISTRY · NOVEMBER 2005

Impact Factor: 4.93 · DOI: 10.1021/cc050077p · Source: PubMed

CITATIONS

31

READS

24

## 5 AUTHORS, INCLUDING:



**Brandon M. Vogel**

Bucknell University

29 PUBLICATIONS 740 CITATIONS

SEE PROFILE



**João T Cabral**

Imperial College London

85 PUBLICATIONS 1,246 CITATIONS

SEE PROFILE



**Balaji Narasimhan**

Iowa State University

203 PUBLICATIONS 2,808 CITATIONS

SEE PROFILE



**Surya K Mallapragada**

Iowa State University

170 PUBLICATIONS 3,005 CITATIONS

SEE PROFILE

## Parallel Synthesis and High Throughput Dissolution Testing of Biodegradable Polyanhydride Copolymers

Brandon M. Vogel,<sup>†</sup> Joao T. Cabral,<sup>‡</sup> Naomi Eidelman,<sup>§</sup> Balaji Narasimhan,<sup>\*,‡</sup> and Surya K. Mallapragada<sup>\*,‡</sup>

*Polymers Division, National Institute of Standards and Technology, Gaithersburg, Maryland 20899, Department of Chemical Engineering and Chemical Technology, Imperial College, London, SW7 2AZ, UK, Paffenbarger Research Center, American Dental Association Foundation, Polymer Division, National Institute of Standards and Technology, Gaithersburg, Maryland 20899, Department of Chemical and Biological Engineering, Iowa State University, Ames, Iowa 50011*

*Received June 16, 2005*

We have demonstrated that polycondensation reactions can be carried out in a combinatorial fashion and that the polymer library can be screened at high throughput using a rapid prototyping technique to fabricate multiwell substrates. A linearly varying compositional library of 100 different biodegradable polyanhydride random copolymers that are promising carriers for controlled drug delivery was designed, fabricated, and characterized by IR microscopy within a few hours. The polyanhydride copolymer library was based on 1,6-bis(*p*-carboxyphenoxy)hexane (CPH) and sebacic anhydride (SA) and was characterized with infrared microspectroscopy to determine the composition within each well. Since degradation and release rates depend on copolymer composition, we also developed new high-throughput methods to investigate drug release from this library of copolymers by designing specific wells for each task. A subset of this library was chosen, and a substrate was designed and fabricated to enable the synthesis and monitoring of dye dissolution from a range of polyanhydride copolymers in a parallel fashion using a CCD camera. Multisample substrates were fabricated with a novel rapid prototyping method that consists of an organic solvent-resistant array of 10 × 10 microwells of 2-μL volume each. The libraries were deposited with a custom-built liquid dispensing system consisting of a series of computer-controlled volume-dispensing pumps and XYZ motion stages. The parallel dye dissolution study displayed a decreasing rate of release with increasing CPH content. This result agrees with previously published data for dye release from poly(CPH-co-SA) copolymers. The methodology described in this work is amenable to numerous applications in the arenas of high-throughput polymer synthesis and characterization.

### Introduction

Polyanhydrides are an important class of hydrolytically degrading biomaterials used for controlled release applications.<sup>1–7</sup> Their characteristic surface erosion behavior (due to their hydrophobic nature) makes them excellent candidates for controlled delivery of drugs and biomacromolecules, such as therapeutic proteins, vaccines, and growth factors. However, polyanhydrides have a few limitations, such as poor processability, low solubility in common solvents, and a tendency to be very hydrophobic.<sup>4,5,8</sup> Another complicating factor arises because polyanhydrides are usually synthesized by melt polycondensation at elevated temperatures under vacuum, making the synthesis cumbersome and slow.<sup>9–11</sup> Moreover, choosing a polymer chemistry that can effectively stabilize a given therapeutic is not trivial and is further complicated by the large parameter space. For instance,

factors that influence polymer degradation, drug release kinetics, and stability are the polymer degradation rate (controlled by the polymer chemistry), the drug loading, and polymer–drug interactions.<sup>4,5,8</sup> Therefore, rapid, high-throughput methods that generate and screen compositional libraries of polyanhydride copolymers may be useful in rapidly developing new materials for controlled release applications.

Recently, a number of papers in the literature have described the combinatorial synthesis of polymers through enzyme-assisted polymerization, microwave polymerization, or by judicious choice of polymerization reaction chemistries.<sup>12–17</sup> However, none of these examples has addressed condensation polymerization reactions on a high-throughput level without the use of a catalyst, deep-well plates that require large solution volumes, or solution polymerizations that have concentration dependence. Additionally, characterization of these polymer libraries requires isolation of the product from the reaction solvent. Furthermore, many of the discrete library preparation methods involve expensive commercial automated multiwell synthesizers that have low upper temperature limits and large sample volume sizes (~13–

\* To whom correspondence should be addressed. E-mails: (B.N.) nbalaji@iastate.edu; (S.K.M.) suryakm@iastate.edu.

<sup>†</sup> Polymers Division, National Institute of Standards and Technology.

<sup>‡</sup> Imperial College, London.

<sup>§</sup> American Dental Association Foundation, Polymer Division, National Institute of Standards and Technology.

<sup>‡</sup> Iowa State University.

100) mL.<sup>12–17</sup> Such large sample sizes present a disadvantage when working with expensive monomers, because large quantities of material are not usually required for most characterization and screening methods. Reactions carried out in microtiter plates have the advantage of very small volumes (<1 mL) but the microtiter plates are typically made out of common plastics, limiting the reaction temperature.

Cabral and Karim have developed microwell plates that can be rapidly produced on glass cover slips by a rapid prototyping process.<sup>18</sup> The material that forms the wells is a UV-curable, optical adhesive that has high thermal stability and good solvent resistance. The unique advantage of these microwells is the transparency of the glass substrate and the ease of prototyping new well designs for specific applications. Additionally, these microwells are stable at the polymerization temperature of the anhydride monomers as described below, which is an issue with several commercially available multiwell plates. The utility of the synthesized libraries may also be broadened because of the ability to use characterization methods not possible with commercially available plates. Therefore, these novel microwell plates are well-suited for high-throughput synthesis and characterization.

In the rational design of delivery vehicles for drugs, it is important to understand that the release of the drug and its stabilization are influenced by a variety of parameters, including polymer chemistry, polymer erosion mechanism, drug–polymer interactions, and drug loading. To develop predictive models for drug stabilization and release, it is important to design methods that will rapidly screen this large parameter space. Currently available USP-approved dissolution apparatuses can simultaneously monitor drug release from eight tablets, each of which weighs ~100 mg. These devices are not conducive for rapid screening, since large amounts of material need to be synthesized for each well. In addition, solvent evaporation becomes an issue when the dissolution time exceeds ~3 days, which occurs with all of the polyanhydrides described in this paper. Thus, there is a need for parallel screening devices for drug delivery that are small enough that the issues due to large sample size and solvent evaporation are obviated.

Herein, we describe the application of fabricated glass microwell plates to the generation and synthesis of polyanhydride random copolymer libraries as well as the fabrication and evaluation of a parallel dye dissolution experiment on a glass slide. To the best of our knowledge, this is the first example of a self-contained, integrated polymer synthesis and nonsampling technique to obtain release kinetics in a high-throughput manner.

### Materials and Methods

All chemicals were purchased from Sigma-Aldrich (St. Louis, MO) with the exception of the NOA 81 resin, which was purchased from Norland Products Inc. (Cranbury, NJ) and used as received. Sebacic acid (SA) prepolymer and 1,6-bis(*p*-carboxyphenoxy)hexane (CPH) were prepared as described elsewhere.<sup>19</sup>

**Multiwell Array Substrate Fabrication.** The substrate arrays were designed and fabricated using a recently

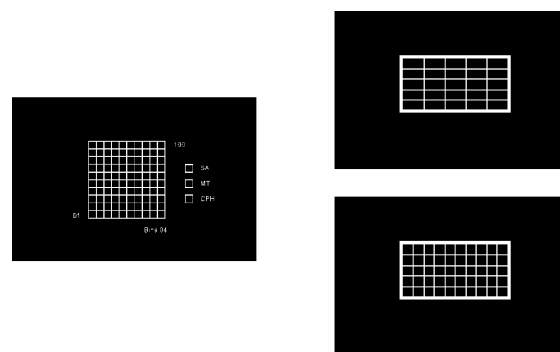


**Figure 1.** A 10 × 10 photomask used to prepare multiwell glass substrates for synthesis (left) and dissolution wells (right) used in this investigation.

developed rapid prototyping technique based on the contact lithography of multifunctional thiolene resins.<sup>20</sup> The photomask was designed with a standard graphics package and printed on a transparency with a 1200-dpi resolution laser printer. It consisted of a 10 × 10 grid (with 300- $\mu$ m line width) and three additional (control) squares, with dimensions commensurate with a glass slide (Figure 1).

A flood 365 nm ultraviolet source (Spectronics, Westbury, NY) imaged the pattern onto a layer of the (negative) photoresist confined between a glass plate and a cured poly-(dimethyl siloxane) (PDMS) surface. A commercially available optical adhesive (NOA 81) was used as the photoresist in this work. The patterned height (and therefore, the well volume) was determined by the administered UV dose in this frontal photopolymerization process.<sup>20</sup> Selective solvents (ethanol and acetone) washed away the unpolymerized material. A feature height of 400  $\mu$ m was fabricated with a 12.0 mJ/cm<sup>2</sup> dose, resulting in 2- $\mu$ L microwells patterned on glass. The whole substrate was then UV-postcured (a flood exposure of an additional 1 J/cm<sup>2</sup>) and thermally cured at 50 °C for 12 h. Dissolution substrates with multiple heights were created using sequential masks to expose the tallest regions for the longest times while providing less exposure to build the shorter features.

**Combinatorial Discrete Library Preparation.** The discrete compositional libraries were fabricated using a liquid dispenser by deposition into the wells of a multiwell substrate. The dispenser consists of a series of syringe pumps (New Era, Farmingdale, NY), an XY stage (composed of two orthogonally stacked linear stages, ILS150CC, Newport, CA), and a motorized actuator along the Z-axis (850G, Newport, CA). The syringes are connected with Teflon tubing to stainless steel needles (gauge 26), which are attached together and secured onto a cured PDMS module (the dispensing “head”). The head is mounted onto a Z-actuator, which is normal to the substrate and aligned with the XY stage. The syringe pumps and the motion stages are connected to a desktop computer and controlled through a LabVIEW (National Instruments, TX) interface. Deposition rates, volumes, and stage motion speeds were controlled. Typical dispensing time per well was 0.3 s. A few binary mixtures of SA prepolymer and CPH prepolymer were prepared using this setup for measurement control (reproducibility) purposes. A typical deposition involved dissolving

the prepolymers or dye in chloroform and placing that solution into a syringe that was used to deposit the library.

**High-Throughput Synthesis of Polyanhydrides.** Prepolymers (CPH-co-SA) of varying compositions were loaded into the discrete library multiwell substrates and placed in a vacuum oven preheated to 180 °C. The prepolymers were allowed to melt before the oven was placed under vacuum and polymerization was allowed to commence. The filled multiwell substrates were polymerized for 1 h before they were removed from the 180 °C oven and placed into a 100 °C oven to minimize thermal stress on the optical adhesive. After the multiwell substrate cooled to 100 °C, the polymer library was placed under vacuum in a desiccator and stored at 4 °C until characterization.

**High-Throughput Characterization of Polymer Libraries with Fourier Transform Infrared Microspectroscopy in Reflectance Mode.** The measurements were performed with a Nicolet Magna-IR 550 FTIR spectrophotometer (Nicolet, Madison, WI) interfaced with a Nic-Plan IR microscope operated in reflectance mode. The microscope is equipped with a video camera, a liquid nitrogen-cooled mercury cadmium telluride (MCT) detector (Nicolet, Madison, WI), and a computer-controlled translation stage (Spectra-Tech, Inc., Shelton, CT) programmable in the *X* and *Y* directions. Although Fourier transform infrared microspectroscopy in reflectance mode (FTIR-RM) was used to quantify the extent of curing for an epoxy library created by a linear temperature gradient,<sup>21</sup> this is the first example (to our knowledge) in which it has been utilized to determine the compositions of a discrete copolymer library. The spectral point-by-point mapping of the copolymer surface in each well was performed with a computer-controlled microscope stage and the Atlus mapping software (Thermo Electron Corp., Madison, WI). Spectral maps of the 10 × 10 wells' specimens were collected at 400- $\mu\text{m}$  intervals along the *x* axis and 400- $\mu\text{m}$  intervals along the *y* axis (total of 3780 spectra) with beam spot size of 400  $\mu\text{m}$  × 400  $\mu\text{m}$ , 48 scans per acquired spectrum and 8  $\text{cm}^{-1}$  resolution in the 650–4000  $\text{cm}^{-1}$  region. Next, the specimen was mapped using 2400- $\mu\text{m}$  steps in both the *X* and *Y* axes (the distance between the centers of the wells) to obtain a map with spectra of the copolymers without the walls of the wells. Subtracting the walls of the wells was necessary to permit automated quantification; otherwise, the spectra due to the walls interfered with the spectra of the individual samples in the wells. Additional spectra were collected from wells that provided incomplete spectra as a result of bare glass or defects in the polymer film. The reflectance spectra were proportioned against a background of a reflective slide and transformed to absorbance spectra using the Kramers–Kronig transform algorithm for dispersion correction, available in Omnic software (Thermo Electron Corp., Madison, WI). The FTIR-RM maps were processed as the areas under the 1605  $\text{cm}^{-1}$  peak of the poly(CPH) aromatic carbons ((1587–1625)  $\text{cm}^{-1}$  spectral region) and the 1815  $\text{cm}^{-1}$  peak of the poly(SA) aliphatic carbons ((1790–1850)  $\text{cm}^{-1}$  spectral region) and displayed as color contour maps.<sup>22</sup> A series of known compositions [0, 80, and 100 mol % CPH-SA] prepared from stock solutions of prepolymers mixed

by hand were placed into wells and polymerized under conditions identical to the aforementioned procedure to provide standards for calibrating the compositions obtained from the spectral maps. Six spectra were collected from each of the calibrated compositions to obtain a calibration curve to quantitatively determine the compositions of the multiwell samples. The spectra collected from the control compositions were imported into the recently revised ISys software (Spectral Dimensions Inc., Olney, MD),<sup>23</sup> and the areas under the 1605  $\text{cm}^{-1}$  peak and the 1815  $\text{cm}^{-1}$  peak were calculated for each spectrum in the same spectral regions used in processing the color contour maps. A calibration curve (linear regression,  $R^2 = 0.983$ ) was constructed from the control compositions by plotting the ratio of the 1605  $\text{cm}^{-1}$  peak area to the sum of the 1605 and the 1815  $\text{cm}^{-1}$  peak areas versus the fraction of CPH in each control copolymer. The calibration curve was constructed following a similar procedure that was used to determine the compositions of a gradient polymer blend.<sup>23</sup> The spectra from the map of the well centers were processed with ISys identical to the calibration standards.

**Nuclear Magnetic Resonance (NMR) Characterization of Polymeric Materials.** Proton nuclear magnetic resonance ( $^1\text{H}$  NMR) was used to verify chemical structure and to determine the degree of polymerization for each polymer and prepolymer. We note that for the range of molecular weights synthesized in these studies, NMR provides a more accurate determination of the molecular weight than does gel permeation chromatography. NMR spectra were taken on a 6.35 T JEOL GX270 spectrometer manufactured by JEOL, Ltd. (Akishima, Japan). A number of copolymers were characterized by  $^1\text{H}$  NMR in deuterated chloroform (99.8% atom-*d*) with the chemical shifts calibrated to the chloroform ( $\delta = 7.26$  ppm) peak. The NMR samples were prepared by hand-mixing compositions and manually depositing the prepolymer solutions onto glass slides. The glass slides with prepolymers were then polymerized at 180 °C under vacuum for 60 min. The polymers were dissolved in chloroform, and a  $^1\text{H}$  NMR was collected for each sample. The degree of polymerization, average monomer segment lengths, and degree of randomness were all calculated from NMR as described previously.<sup>24–26</sup>

**Dissolution Device Fabrication.** As mentioned previously, dissolution wells consisting of 25 samples were fabricated on glass slides using commercially available optical adhesive. The dissolution wells were designed such that a polymer film could be placed within to enable parallel characterization of the dissolution medium without needing resupply or sampling of the dissolution medium. Each well was rectangular (3 mm × 6 mm) in shape with an inner bisector that created two equal sized squares (3 mm × 3 mm). The height of the rectangle was fabricated (~900  $\mu\text{m}$ ) with the inner bisector one-third of this height (300  $\mu\text{m}$ ), resulting in a well that contained a total of 16.2  $\mu\text{L}$  of liquid. The well was rectangular to enable imaging of the dye in the dissolution medium as well as in the polymer film with the use of a CCD camera to detect fluorescence intensity (FI). If the polymer film has a fluorescent dye distributed within it, then the CCD camera will detect the dye within



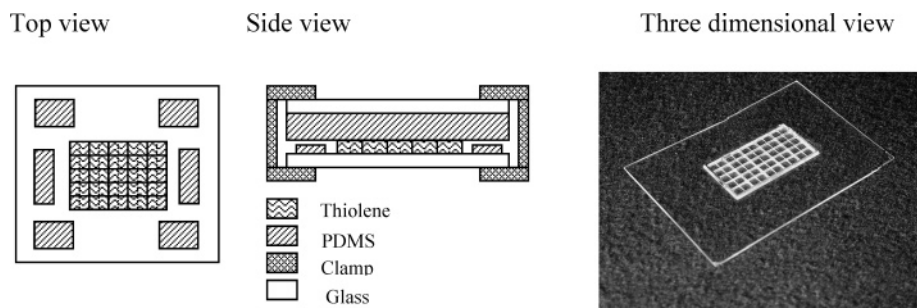


**Figure 2.** Schematic of the parallel dissolution device.

the polymer film plus the dye dissolved within the dissolution media above the film. Therefore, the half of the rectangle that does not contain the film could be “sampled” to determine the FI of the dissolution media without the polymer film/dye background. The dissolution device consisted of a glass slide modified with the rectangular wells surrounded by a 750- $\mu\text{m}$ -thick cross-linked poly(dimethylsiloxane) (PDMS) gasket. To enclose the wells, a 3-mm-thick slab of PDMS backed with another glass slide was laid over the top of the wells and clamped together to form a physically sealed device, as shown in Figure 2.

The top PDMS layer acted as a conformal sealant to enclose the wells and allow the dissolution to occur. The PDMS gasket around the outside of the wells was used to minimize the stress on the glass slide during the clamping process. The PDMS gasket prevents the glass slides from bending too far, thus resulting in lower stresses applied to the slides.

**CCD Imaging of the Dissolution Wells and Release Kinetics.** Release kinetics of ethidium bromide bisacrylamide were monitored using the VersaDoc 3000 imaging system with Quantity One 1-D image analysis software (BioRad Laboratories, Hercules, CA). The images were taken using a 20–40-mm Tamron zoom lens with a 660-nm cutoff filter over the lens. The VersaDoc was configured to use broadband UV excitation ( $\lambda_{\text{em}} = 265\text{--}365\text{ nm}$ ) with a 520 low-pass emission filter.

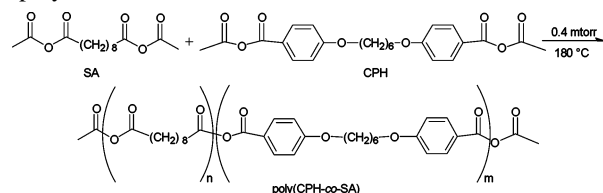
Polyanhydride copolymers that were synthesized with nonreactive ethidium bromide bisacrylamide ( $\lambda_{\text{ex}} = 304\text{ nm}$ ) were imaged at time points to determine the FI of the release medium (0.1 mol/L phosphate buffer solution pH = 7.4) and polymer film. Image analysis was used to determine FI (peak intensity of well) at a given time point. A program was written using Igor Pro (Wavemetric, Lake Oswego, OR) to automate the image analysis.

**Spectral Assignments. Poly(sebacic anhydride).**  $^1\text{H}$  NMR ( $\text{CDCl}_3$ ):  $\delta = 1.3$  (m, H8), 1.65 (m, H4), 2.2 (s, H6 acetyl end), 2.3 (t, H2  $\alpha$  to acid end), 2.4 (m, H4  $\alpha$  to SA-SA).

**Poly[1,6-bis(*p*-carboxyphenoxy)hexane].**  $^1\text{H}$  NMR ( $\text{CDCl}_3$ ):  $\delta = 1.5$  (m, H4), 1.7 (m, H4), 2.2 (s, H6 acetyl end), 4.1 (m, H4), 6.95 (d, H4), 8.0 (d, H4 CPH end), 8.1 (d, H4 CPH-CPH).

**Poly[1,6-bis(*p*-carboxyphenoxy)hexane-co-sebacic anhydride].**  $^1\text{H}$  NMR ( $\text{CDCl}_3$ ):  $\delta = 1.35$  (m, H8), 1.6 (m, H4), 1.7 (m, H4), 2.2 (s, H6), 2.3 (s, H6), 2.4 (t, H4  $\alpha$  to SA-SA), 2.6 (t, H4 SA-CPH), 4.1 (m, H4), 6.95 (d, H4), 8.0 (d, H4 CPH-SA), 8.1 (d, H4 CPH-CPH).

**Scheme 1.** Reaction of Two Acetylated Diacid Prepolymers (SA and CPH) to Form a Polyanhydride Random Copolymer<sup>a</sup>



<sup>a</sup> The monomers were chosen because of their common use in controlled drug delivery as well as their ability to degrade over a reasonable time period.<sup>4,5,10</sup>

## Results & Discussion

**Polyanhydride Libraries.** Fabricated multiwell substrates were filled with SA and CPH prepolymers in compositions ranging from 0 to 100 mol % SA. The prepolymers were subsequently melt-polymerized at 180 °C under high vacuum to yield polyanhydride random copolymers (Scheme 1).

Figure 3a shows a visual image of the postpolymerization polyanhydride multiwell substrate taken with the FTIR-RM microspectroscope in the same focal plane as the FTIR-RM spectra were collected. Figure 3b shows IR spectra collected from well nos. 1, 25, 50, 75, and 100. It can be observed that the CPH peak ( $1605\text{ cm}^{-1}$ ) increases with well number and the SA peak ( $1815\text{ cm}^{-1}$ ) decreases with well number, thereby qualitatively confirming the existence of a gradient in copolymer composition with well number.

One distinct observation that can be made from Figure 3a is that the polymers are all contained within a given well and laying quite flat. There is some unevenness or cracking of some of the wells due to thermally induced delamination, but this was only observed in a few wells. FTIR-RM was used to determine qualitative as well as quantitative information about the compositional makeup of each well. The results from a typical IR map are shown in Figure 3c and d. The false color maps with regions of more red indicate more of a given component (red is the highest and blue is the lowest). For instance, the CPH map (Figure 3c) has more pockets of yellow/red toward the top of the substrate, indicating a larger mole percentage of CPH monomer within the copolymers in these wells. Note that the intent was to create a linear gradient of increasing concentration of CPH (and decreasing concentration of SA) in the copolymers from well no. 1 to well no. 100. The nonuniformity of the colors in some of the wells in the maps arises from spectra taken on bare spots of the glass substrate instead of the polymer or an uneven polymer surface (see, for example, the defects in wells 71, 81, and 91 in the visual map in Figure 3a and

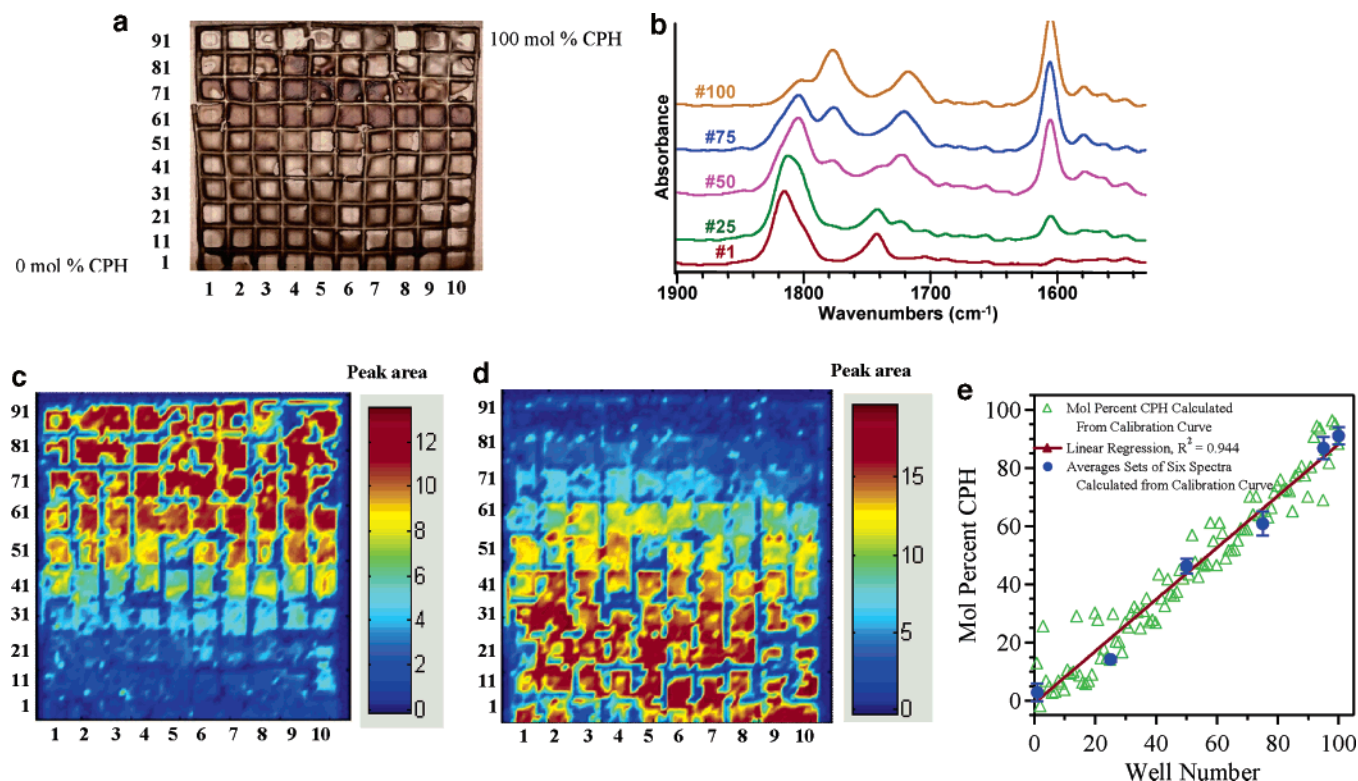


**Figure 3.** (a) Visual map (composed of 2132 boxes, 622  $\mu\text{m} \times 466 \mu\text{m}$  each) of a polyanhydride random copolymer-filled multiwell substrate (post polymerization) with varying composition from 0 to 100 mol % SA and CPH (numbers designate composition of row and column nearest edge). (b) IR spectra of wells nos. 1, 25, 50, 75, and 100. (c, d) IR maps of CPH and SA in the multiwell substrate (left and right) shown in (a). (e) Mol % CPH in each well in (a), as calculated from the FTIR spectra with the calibration curve. The six sets of averages and error bars ( $n = 6$ ) are of spectra that were extracted manually from six wells in the IR maps.

the distribution of the colors in these wells in the CPH map in Figure 3c). Uneven films may cause multiple focal planes in the region the spectrum was collected from and, therefore, result in distorted spectra. However, the general trend of composition of a given monomer increasing is clear from inspection of both IR maps. A more quantitative trend is clearly seen in Figure 3e. The mole percent CPH values in Figure 3e were acquired from only one spectrum of 400  $\times$  400  $\mu\text{m}^2$  out of an area of about 1700  $\times$  1700  $\mu\text{m}^2$ . Therefore, the composition fluctuations were high, and negative values resulted in some cases. However, a linear trend in the composition (as programmed) from well no. 1 to well no. 100 is evident. Currently, the large FTIR maps, which are dispersion-corrected, cannot be processed adequately with the combination of the software packages used. Therefore, sets of six spectra were extracted manually from six wells and processed as those used for the calibration curve. Their averages and standard deviations were overlaid on the curve in Figure 3e, and significantly fewer fluctuations were seen.

<sup>1</sup>H NMR was used to validate the existence of polymers instead of oligomers; to verify the purity of the polymers; to calculate number average relative molecular mass; and to determine the monomer sequence distribution for the compositions, 0, 20, 50, 80, and 100 mol % CPH-co-SA. Figure 4 shows the stacked NMR spectra of the above compositions, in which no peaks corresponding to unreacted diacid are observed, thus confirming the purity of the samples. The degree of polymerization, average monomer segment lengths, and degree of randomness were all calculated from NMR

as described previously.<sup>24–26</sup> Table 1 shows the number average relative molecular mass ( $\overline{M}_n$ ) along with degree of polymerization and degree of randomness calculations for the copolymers.<sup>26</sup>

The degree of randomness is a measure of “blockiness” of the copolymer. Table 1 indicates that the parallel synthesis method described here resulted in high molecular mass polymers, with number average relative molecular mass comparable to those obtained by conventional melt polycondensations.<sup>4,26</sup> Values for the degree of randomness  $< 1$  are more blocklike, whereas values  $> 1$  denote random copolymer behavior. It is well-known that both CPH and SA monomers have reactivity ratios of 1;<sup>26</sup> simply stated, they form random copolymers when copolymerized with another anhydride. The degree of randomness calculation confirms that the copolymers formed by the parallel polycondensation method are random. These results agree with previously published values for the degree of randomness from the poly(CPH-co-SA) system obtained by conventional polymerization techniques under vacuum (Figure 5).<sup>26</sup>

It should be noted that the copolymers with asymmetric monomer feeds (80–20, 20–80) have longer sequence lengths of the component in excess, which is more blocklike. This behavior has also been demonstrated previously for the conventional melt polycondensation of poly(CPH-co-SA).<sup>4,26</sup> Additional “on-chip” characterization methods that can be performed to provide more detailed information on microstructure and phase behavior include small-angle X-ray scattering and scanning probe microscopy.

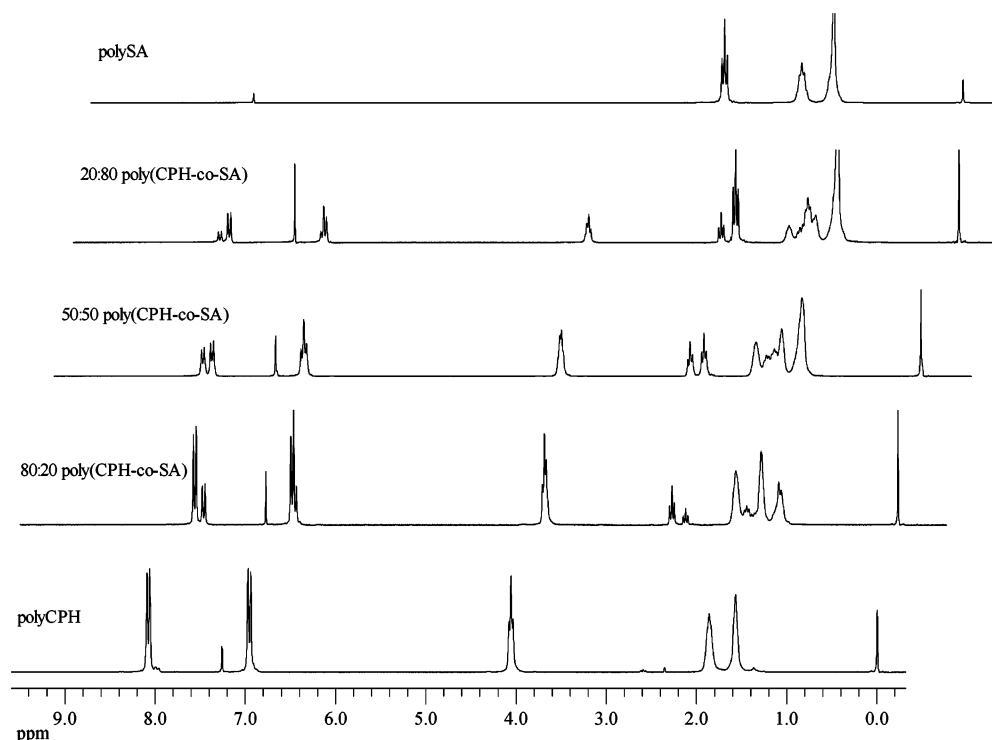


**Figure 4.** Stacked  $^1\text{H}$  NMR spectra of CPH-*co*-SA copolymers (0, 20, 50, 80, 100% CPH) synthesized combinatorially.

**Table 1.** Number-Average Relative Molecular Mass of Copolymers Polymerized in Parallel<sup>a</sup>

| copolymer    | DP | $\bar{M}_n$ (g/mol) | degree of randomness |
|--------------|----|---------------------|----------------------|
| CPH-SA 0–100 | 53 | 9,697               |                      |
| CPH-SA 20–80 | 66 | 14,438              | 1.24                 |
| CPH-SA 50–50 | 71 | 18,763              | 1.01                 |
| CPH-SA 80–20 | 43 | 13,465              | 1.14                 |
| CPH-SA 100–0 | 91 | 32,438              |                      |

<sup>a</sup> All samples were polymerized for 60 min at 180 °C under vacuum.

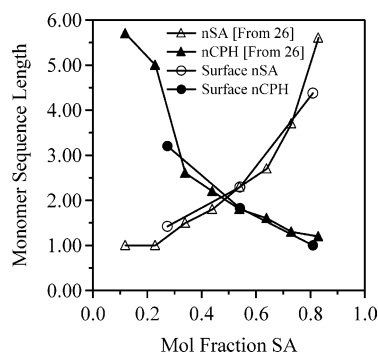


**Figure 5.** Monomer sequence length as a function of copolymer composition in poly(CPH-*co*-SA) polymerized conventionally (from literature<sup>26</sup>) and vacuum oven conditions. The included lines between points are to guide the eye.

**Dissolution Screening.** Five compositions of poly(CPH-*co*-SA) random copolymers were synthesized (with nonre-active ethidium bromide bisacrylamide added) within rows of the dissolution wells. We chose to replicate each composition five times to obtain better statistics instead of synthesizing extra compositions. Certainly, fabricating larger numbers of arrays is possible and easily achieved if more compositions or replicates are desired. It should be noted that many microscale parallel dissolution apparatuses could be loaded,

synthesized, and tested simultaneously. As for the dissolution apparatuses, high temperatures (> 160 °C) caused delamination of the thiolene resin from the glass substrate. This problem was much more noticeable for the dissolution wells, as compared to the synthesis wells most likely due to the larger features (height) of the dissolution wells. The larger features likely contain residual stresses or thermal gradients when heated, causing a stress gradient, resulting in delamination. To avoid this issue, samples were polymerized on Kapton films at 180 °C under vacuum. The Kapton film has excellent thermal stability as well as chemical inertness to not only chloroform but also diacid and anhydride functionality. After polymerization, small 2-mm disks were punched out of the Kapton/polyanhydride films using a tissue punch. The round polyanhydride films were then fixed into place within a given column of the dissolution device with an adhesive. Phosphate buffer saline (0.1 mol/L, pH = 7.4) was added to the wells, and the device was closed.

An attractive feature of this technique is the ability not only to follow dye release into the release medium but also to determine the dye content in the polymer samples as a function of time. Images were collected from selected time points, and data was extracted using a program written in Igor (Figure 6). The program generates a region of interest (ROI) on the image (i.e., within a well) and determines the average gray scale from the ROI. This operation was repeated 50 times (once for each well), and the data from each column (same compositions) was averaged to provide a time point. After several images (time points) were fed into the program, release curves were generated. It should be noted that the FI in the dissolution medium was subtracted from the FI of the polymer film to remove any excess fluorescence adding to the film FI from the release medium. There are some subtle fluctuations in the release curves at all compositions for some



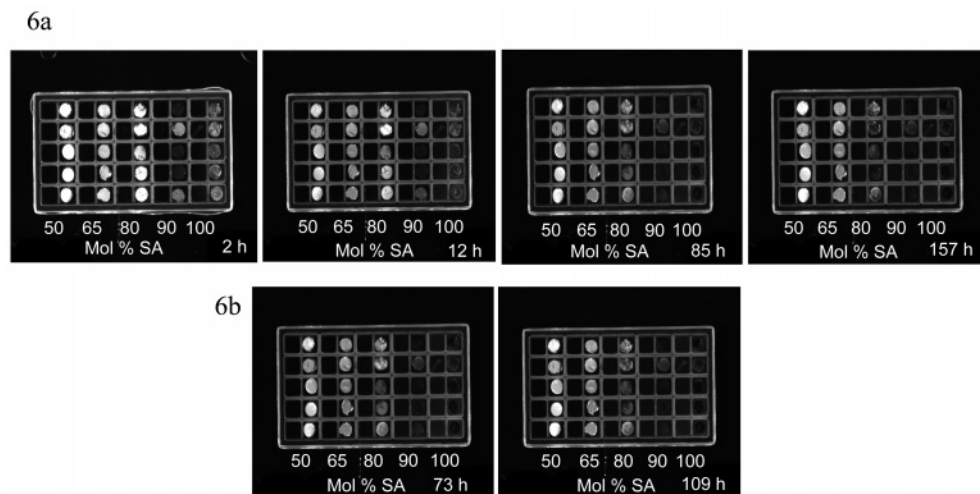


**Figure 6.** Image of the dissolution device during the experiment. (a) Notice the dye within the polymer films (right columns) and the dye releasing (left columns) for 2-, 12-, 85-, and 157-h times. Compositions of the polymers are marked on the image for clarity. (b) Dissolution images showing fluctuations in FI for time points 73 and 109 h. Notice the increase in FI in the polymer film from 73 to 109 (column 4, row 4).

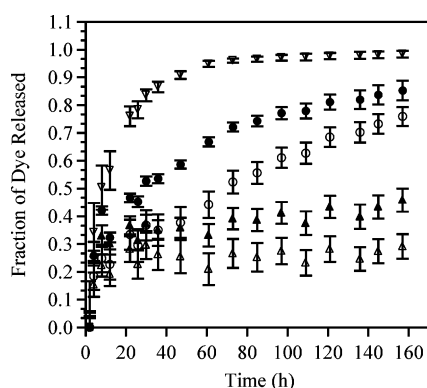


**Figure 7.** Release data collected from the high-throughput dissolution experiment. All time points consist of an average ( $n = 5$ ). The error bars are measures of absolute uncertainty calculated by error propagation. From top to bottom, the values are increasing in CPH content from 0, 10, 20, 35, 50 mol % CPH.

time points (73 h, for instance); this may be a result of systematic error from fluctuation in exposure during the data collection (see Figure 6b).

One way to alleviate this problem would be to image a constant calibration curve at each time point to correct for these differences. The release of the dye was actually followed by the change in FI of the polymer film/dye, because the dye in the release medium was too dilute to follow accurately. The FI of individual columns varies due to differences in the film thickness. As a result, there is more total dye within the thicker films (for example, 50 mol % SA versus 100 mol % SA in Figure 6a). However, there are visible differences in FI for different times, as shown in Figure 6a. The quantitative results from the high-throughput dissolution experiment are shown in Figure 7.

The fraction of dye released was calculated by normalizing the FI from the zero-time point. The release of ethidium bromide bisacrylamide from the five copolymers of CPH-SA varied depending on the composition, with poly(SA) releasing the fastest and the 50–50 CPH-SA copolymer releasing the slowest. This is expected because the hydrophobicity of the copolymer increases with CPH content.

Burst release occurred from the poly(SA) homopolymer, whereas the release profile was almost zero order from the 10–90 and 20–80 mol % CPH-SA copolymers. The burst of dye from the poly(SA) is likely caused by poor polymer–dye compatibility, which results in a dye distribution within the polymer that is preferentially toward the polymer surface. This burst becomes smaller as the CPH content in the copolymer is increased and the release profiles become near zero-order. This type of behavior is consistent with release data reported by Shen et al. for the same CPH-SA copolymer system for the release of disperse yellow 3 and *p*-nitroaniline from disks tested using conventional sampling methods.<sup>4</sup> These model dyes are similar to ethidium bromide bisacrylamide in size, and the release rates observed in both the high-throughput and conventional studies show excellent agreement.

The high throughput drug release studies described herein can be used to draw important inferences that will aid in the rational design of drug delivery vehicles. For example, from the studies shown in Figure 7, conclusions can be drawn about drug–polymer compatibility as a function of polymer chemistry based on the drug release profile (e.g., burst effect vs zero-order release) and drug release and polymer degradation rates that will enable tailoring the right chemistry for the appropriate application.

## Conclusions

We have demonstrated that polycondensation reactions can be carried out in a combinatorial fashion by synthesizing 100 different polyanhydride random copolymers in 60 min. The library was readily characterized and calibrated with infrared microscopy. Additionally, a device for high-throughput dissolution screening was fabricated through a photolithographic rapid prototyping method and tested. The library was readily characterized and calibrated with infrared microscopy. The release of ethidium bromide bisacrylamide was followed by imaging the dissolution array and performing image analysis to extract the release profiles. These methods can be potentially extended to synthesize and



evaluate the dissolution profiles of thousands of copolymers, with varying compositions at a time, thereby facilitating the screening of polymers for controlled drug delivery applications.

**Acknowledgment.** We thank the Institute for Combinatorial Discovery, the Institute for Physical Research and Technology at Iowa State University, the NIST Combinatorial Methods Center, the American Dental Association Foundation and the Whitaker Foundation for financial support. We also thank Newell R. Washburn and Michael Weir for valuable discussions and assistance.

## References and Notes

- (1) Domb, A. J.; Langer, R. *J. Polym. Sci., Part A: Polym. Chem.* **1987**, *25*, 3373–3386.
- (2) Cleland, J. L.; Daugherty, A.; Mrsny, R. *Curr. Opin. Biol.* **2001**, *12*, 212–219.
- (3) Larobina, D.; Mensitieri, G.; Kipper, M. J.; Narasimhan, B. *AIChE* **2002**, *48*, 2960–2970.
- (4) Shen, E.; Kipper, M. J.; Dziadul, B.; Lim, M.-K.; Narasimhan, B. *J. Controlled Release* **2002**, *82*, 115–125.
- (5) Kipper, M. J.; Shen, E.; Determan, A.; Narasimhan, B. *Biomaterials* **2002**, *23*, 4405–4412.
- (6) Kumar, N.; Langer, R. S.; Domb, A. J. *Adv. Drug Delivery Rev.* **2002**, *54*, 889–910.
- (7) Kumar, N.; Albertsson, A.-C.; Edlund, U.; Teomim, D.; Rasiel, A.; Domb, A. J. *Biopolymers* **2002**, *4*, 203–234.
- (8) Vogel, B. M.; Mallapragada, S. K. *Biomaterials* **2005**, *26*, 721–728.
- (9) Domb, A. J.; Amselem, S.; Shah, J.; Maniar, M. *Adv. Polym. Sci.* **1993**, *107*, 93–141.
- (10) Domb, A. J.; Elmalak, O.; Shastri, V. R.; Ta-Shma, Z.; Masters, D. M.; Ringel, I.; Teomim, D.; Langer, R. *Drug Targeting Delivery* **1997**, *7*, 135–159.
- (11) Leong, K. W.; Brott, B. C.; Langer, R. *Biomed. Mater. Res.* **1985**, *19*, 941–955.
- (12) Brocchini, S.; James, K.; Tangpasuthadol, V.; Kohn, J. *Biomed. Mater. Res.* **1998**, *42*, 66–75.
- (13) Kim, D. Y.; Dordick, J. S. *Biotechnol. Bioeng.* **2001**, *76*, 200–206.
- (14) Lynn, D. M.; Anderson, D. G.; Putnam, D.; Langer, R. *J. Am. Chem. Soc.* **2001**, *123*, 8155–8156.
- (15) Anderson, D. G.; Lynn, D. M.; Langer, R. *Angew. Chem., Int. Ed.* **2003**, *42*, 3153–3158.
- (16) Akinc, A.; Lynn, D. M.; Anderson, D. G.; Langer, R. *J. Am. Chem. Soc.* **2003**, *125*, 5316–5323.
- (17) Vogel, B. M.; Mallapragada, S. K.; Narasimhan, B. *Macromol. Rapid Comm.* **2004**, *25*, 330–333.
- (18) Cabral, J. T.; Karim, A. *Meas. Sci. Technol.* **2005**, *16*, 191–198.
- (19) Conix, A. J. *Macromol. Synth.* **1966**, *2*, 95–99.
- (20) Cabral, J. T.; Hudson, S. D.; Harrison, C.; Douglas, J. F. *Langmuir* **2004**, *20*, 10020–10029.
- (21) Eidelman, N.; Raghavan, D.; Forster, A. M.; Amis, E. J.; Karim, A. *Macromol. Rapid Commun.* **2004**, *25*, 259–263.
- (22) Mathiowitz, E.; Kreitz, M.; Pekarek, K. *Macromolecules* **1993**, *26*, 6749–6755.
- (23) Eidelman, N.; Simon, C. G. *J. Res. Natl. Inst. Stand. Technol.* **2004**, *109*, 219–231.
- (24) Bovey, F. A. *Chain Structure and Conformation of Macromolecules*; Academic Press, Inc.: New York, 1982.
- (25) McCann, D. L.; Heatley, F.; D'Emanuele, A. *Polymer* **1998**, *40*, 2151–2162.
- (26) Ron, E.; Mathiowitz, E.; Mathiowitz, G.; Domb, A.; Langer, R. *Macromolecules* **1991**, *24*, 2278–2282.

CC050077P